Cavitation as a Working Mechanism of the Er,Cr:YSGG Laser in Endodontics: A Visualization Study

Jan W. Blanken[a,b], Rudolf M. Verdaasdonk[b]

[a] *Research Associate, Department of Medical Physics, University Medical Center, Utrecht, The Netherlands; Dentist in Private Practice, Utrecht, The Netherlands.*
[b] *Clinical Physicist, Department of Medical Physics, University Medical Center, Utrecht, The Netherlands.*

Purpose: The objective of this study was to obtain a better understanding of the working mechanism of the Er,Cr:YSGG laser in endodontics using specialized imaging techniques.

Materials and Methods: Using a high-speed imaging setup, cavitation bubbles induced by Er,Cr:YSGG laser were visualized with high temporal and special resolution in a water environment and in glass models of root canals using silica tips of 200, 320, and 400 µm diameter. A thermal imaging technique was combined with thermocouples to measure the temperature increase in the canal wall.

Results: In water, the cavitation bubbles were reproducible. The relationship between pulse energy and dimensions of the bubble is linear. However, the dynamics of cavitation bubbles in the root canal model is complex. The cavitation effects exist for a much longer period of time and there is a turbulent mixture with air or gas bubbles. Colored dyes show very fast fluid motion in and out of the canal during laser exposure. The temperature increase measured was only 5 to 10 degrees.

Conclusion: Our imaging suggests that the working mechanism of an Er,Cr:YSGG laser in root canal treatment can be attributed to cavitation effects inducing high speed fluid motions into and out of the canal. This might effectively remove the smear layer and sterilize the canal wall. The thermal component is moderate.

Keywords: laser, cavitation, endodontics, Er,Cr:YSGG, fluid dynamics.

J Oral Laser Applications: 2007; 7: 97-106. *Submitted for publication: 16.01.07; accepted for publication: 12.02.07.*

Many laser systems, both continuous wave and pulsed, have been studied in terms of their usefulness in endodontic therapy. Most studies focused on bactericidal capacities, removal of the smear layer, and thermal safety.

In vitro studies have shown that several wavelengths have bactericidal effects.[1-3] Some pulsed lasers are also able to remove the smear layer. It is likely that this ability is based on photothermal effects, because in many studies, the laser systems were used in air, sometimes in combination with air/water cooling.[4] Thermal effects were studied in vitro, and under controlled conditions many lasers proved to be safe.[5]

The Er:YAG and Er,Cr:YSGG lasers have been studied especially for their capacity to clean the root canal walls after conventional root canal preparation. Even with high power settings using an Er,Cr:YSGG laser with water cooling, thermal effects were moderate and within limits regarded to be safe. Undesired side effects such as ledging and carbonization were almost absent. Although the diameter of the fiber used was 750 µm and the canals were instrumented up to file 80, energies up to 250 and 300 mJ at 20 Hz were applied safely. After laser use, root canal walls proved to be free from the smear layer.[6]

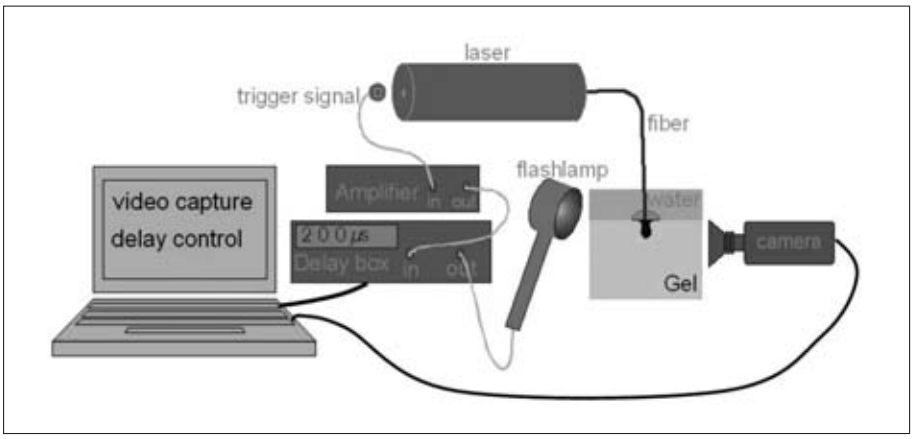

Fig 1 Optical setup.

Using fibers of 200 and 320 µm and pulse energies of 100 and 150 mJ at 20 Hz, partial absence of debris and smear layer were found, as were open tubules.[7]

What happens inside a root canal using an Er,Cr:YSGG laser is only briefly and hypothetically discussed in the literature. Some authors state that absorption of the radiation by water in the smear layer and debris causes a rapid temperature rise and therefore a kind of explosive removal.[8,9]

This study aims to evaluate the contribution of cavitation effects using the Er,Cr:YSGG in a root canal that is filled with water or when an air/water spray is used.

Cavitation effects can be generated in various ways.

1) By moving an object at high speed through a liquid, a gap can be formed behind the object, leaving a vacuum. This cavity is filled by surrounding fluid. Due to the low pressure, the incoming liquid is accelerated, creating forceful microjets focused on the center of implosion or nearby surfaces. These implosions are so forceful that they can erode metal surfaces, as observed on the surface of propellers of ships, pumps and pipes.
2) Using ultrasound, pressure waves can be induced in liquid. At the low pressure phase of the wave, the liquid starts boiling at room temperature. The low pressure phase is usually not maintained and the bubble implodes, creating the high-speed liquid motion as mentioned before. Again, the pressure and forces at the center of implosion are very high. This mechanism is used to accelerate chemical reactions or even nuclear fusion.[10]
3) By instantly heating a liquid to boiling temperature, high pressure vapor is formed that expands at high speed. The momentum of expansion slows down as the pressure and temperature, and the pressure of the surrounding liquid, revert to an implosion. The pressure inside the cavity might drop far below ambient pressure. The surrounding liquid accelerates inward, create high intensity microjets focused on the center of implosion or nearby surfaces.

Pulsed lasers interacting with fluid (water) can also create cavitation bubbles. This has been described for many lasers, such as the ruby, excimer, Q-switched Nd:YAG, Ho:YAG, and Er:YAG. Using piezoelectric transducers, very high pressure waves were measured at the moment of expansion and especially the moment of implosion.

These cavitation effects have been described as the mechanism of action for various medical laser applications, eg, in ophthalmology to treat secondary cataracts using a focused q-switched Nd:YAG laser, and in urology for lithotripsy to crush bladder stones using the Holmium laser.

This study aims to provide evidence that cavitation effects have a major contribution to the mechanism of action of the Er,Cr:YSGG laser in the treatment of root canals.

MATERIALS AND METHODS

High-speed Imaging Setup

Cavitation and vapor bubble formation is a fast process that evolves mainly in the range of 1 microsecond to 1 millisecond. Normally, a highly specialized and expensive camera system would be needed, capable of capturing many thousand frames within one second.

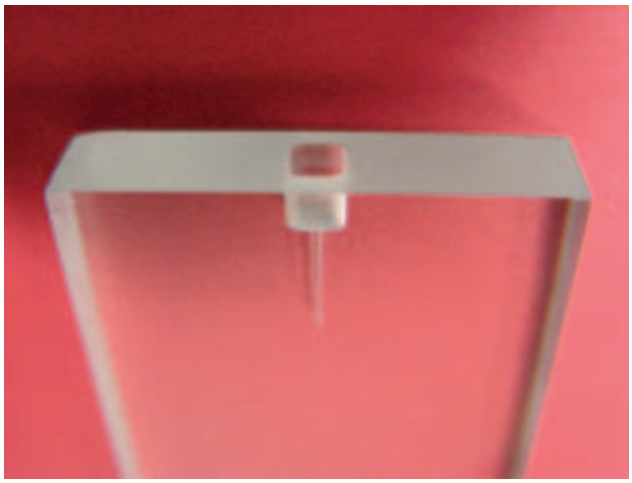

Fig 2 Glass block with root canal and artificial pulp chamber.

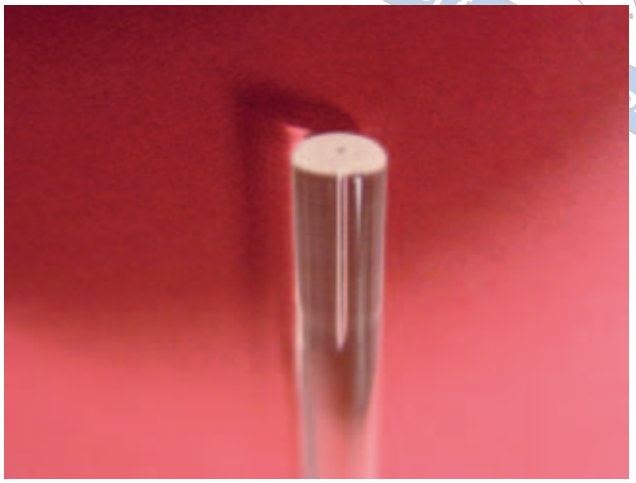

Fig 3 Glass tube with artificial root canal.

However, in vitro under controlled conditions, many experiments can be repeated and are reproducible. Therefore, an alternative high-speed imaging technique was applied in this study that was developed and described by Verdaasdonk et al.[13,14] With this method, laser/tissue interaction is visualized in real time by capturing images at preset delays during the course of action.

The optical setup is shown in Fig 1. At the onset of a laser pulse from an Er,Cr:YSGG laser (Waterlase Millenium, Biolase Technology; San Clemente, CA, USA, 2780 nm, 20 Hz, maximum pulse energy 300 mJ), a signal was sent through an amplifier and a programmed time-delay box to trigger a flash lamp (Portable stroboscope Type 4912, maximum 200 Hz) (Brüe & Kjaer; Naerum, Denmark). The light flash of 2 µs (FWHM) was aimed at the target at specific angles to obtain maximum contrast. At the same time, a CCD camera (C-cam technologies BC 1 15-u-B -40, Vector International; Leuven, Belgium) was triggered to capture an image of the target with the time resolution of the flash (2 µs). The delay box was programmed to extend the delay at each consequent laser pulse with preset steps of 1 µs minimum up to ms. At the pulse frequency of the laser (20 Hz), images were captured to an avi or mpeg movie sequence, showing the dynamics of interaction of the laser pulse in the range of 1 to 1000 µs with 2 µs resolution. To test the reproducibility, more images were captured at each delay time. The laser was modified to shut off the aiming beam which would interfere with the imaging.

By video editing these recordings (Mpeg Video Wizard Womble Multimedia; Cupertino, CA, USA), movies and snap shots could be produced of the cavitation bubbles during their life cycle with a time resolution down to 1 µs.

Root Canal Models

To simulate and visualize the conditions within a root canal, either a glass cylinder or a glass block with a lumen shaped like a root canal were used (Figs 2 and 3). The inner diameter at the apex was 400 µm; the taper was 0.06 mm and the length of the canal 15 mm. To create controlled conditions, the glass models were submerged in water while making the recordings to prevent interference from air. The canal was filled with water or a red colored dye and remaining small air bubbles were removed as thoroughly as possible. The water was degasified to prevent the formation of gas bubbles during the experiments.

Fiber Tips

Fiber tips made of silica, with diameters of 200, 320 and 400 µm and lengths of 25.28 and 33 mm as are used in endodontic treatment, were supplied by the manufacturer. The fiber tips were fixed in the hand piece of the Er,Cr:YSGG laser and positioned above the water container. The tip was either submerged in water or put into the root canal model.

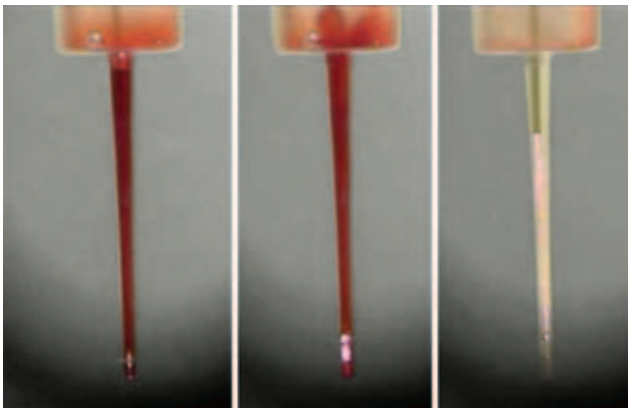

Fig 4 The left panel shows the root canal model filled with red dye and clear fluid on top in the artificial pulp chamber. At the first few laser pulses (125 mJ at 20 Hz), a cloud of red dye ejects into the pulp chamber (middle panel). After 3 s, the red dye in the canal has been replaced by clear fluid (right panel).

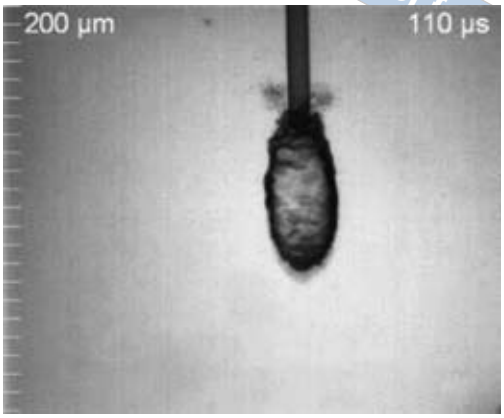

Fig 5 Example of a captured image of an expanding bubble.

Experiments

The high-speed imaging was performed with 200, 320 and 400 µm diameter tips submerged in water. Video sequences were recorded of bubble expansion and implosion in a time range of 10 µs to 1000 µs, typically with steps of 10 µs. The pulse energy ranged from 12.5 mJ to 250 mJ at 20 Hz (0.25 W to 5 W). The pulse energies have to be corrected for energy loss with a calibration factor of 0.3 for the 200-µm, 0.6 for the 320-µm, and 0.75 for the 400-µm fibers according to the manufacturer's information.

In the same way, the bubble dynamics in the root canal model were recorded. However, only 200-µm fibers were used.

RESULTS

Basic Canal Experiment

To simulate what happens when a root canal is treated using a 200-µm fiber with water spray, close-up video recordings were made. Firstly, the fiber was inserted into a dry canal, and at the start of the water spray from the handpiece, the canal filled with water instantly.

Assuming the root canal would normally be filled with fluid during treatment, it was filled with red dye for the next experiment, showing the exchange of fluid. During exposure with pulse energies above 75 mJ, the dye was removed from the root canal within seconds, as illustrated in Fig 4.

Erbium Laser-induced Bubble and Cavitation Dynamics in Water

With the fiber tips submerged in degasified water, video sequences were recorded of bubble expansion and implosion in a time range of 10 µs to 1000 µs, with typical steps of 10 µs.

Figure 5 shows an example of a captured image at high resolution of an expanding bubble. In each image, information on the size and delay from the start of the laser pulse was recorded and displayed.

These individual images at each delay time can be combined into a sequence, as shown in Fig 6, showing the dynamics during the lifetime of the expanding and imploding bubble.

Typically, the dynamics of the bubble induced by the Er,Cr:YSGG laser in water can be described as follows:

The Er,Cr:YSGG laser emits its energy in pulses about 130 µs long. At the beginning of the laser pulse (0 to 50 µs), the energy is absorbed in a 2-µm layer that is instantly heated to boiling temperature and turned into vapor. This vapor at high pressure starts expanding at high speed and provides an opening in front of the fiber for the erbium light. As the laser continues to emit energy, the light passes through the bubble and evaporates the water surface at the front of

Fig 6 Captured images of expanding and imploding vapor bubble at 0, 30, 50, 60, 70, 90, 110, 130, 150, 165, 180, 200, 230 and 260 µs after the onset of 50 mJ pulses.

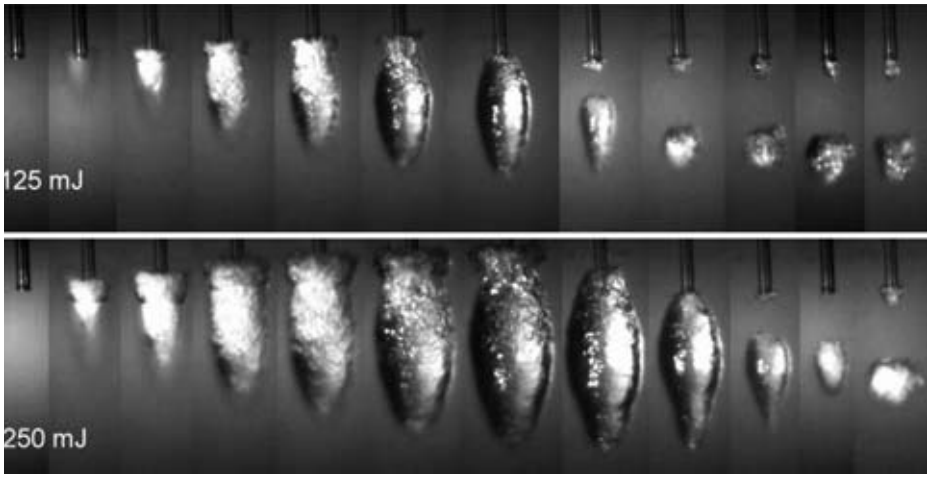

Fig 7 Captured images of expanding and imploding vapor bubble induced by 125 mJ (top) and 250 mJ (bottom) pulses at 20 Hz. The sequences of frames from left to right show the dynamics in time after start of the pulse at 0, 25, 50, 80, 100, 150, 205, 265, 320, 355, 375 and 400 µs.

the bubble. In this way, it "drills" a channel through the liquid until the pulse ends after about 140 µs. This mechanism has been referred to as "the Moses effect in the microsecond region" by van Leeuwen.[15] As the energy source stops, the vapor cools and starts condensing, while the momentum of expansion creates a lower pressure inside the bubble. Both mechanisms provoke an implosion of the bubble. Liquid surrounding the bubble is accelerated to fill in the gap. Near the fiber tip, where the expansion started, the bubble implosion begins, first resulting in separation the bubble from the fiber. Consequently, the water seems to rush into the bubble from the back, making the imploding bubble shaped like a sickle. After 260 µs, the process of implosion is finished and the bubble has vanished. This bubble mechanism has shown to be reproducible at each pulse in a free water environment.

The dynamics of the bubble in relation to fiber diameter and pulse energy was obtained from sequences of high-speed images for 200, 320, and 400 µm diameter tips and for pulse energies ranging from 12.5 mJ to 250 mJ at 20 Hz (0.25 W to 5 W).

A representative series is shown in Fig 7, comparing pulse energy settings of 125 and 250 mJ.

From the high-speed imaging, quantitative data were abstracted regarding the dimensions of the bubbles in relation to energy and fiber diameter, as presented in Fig 8. The length of the bubble increases linearly for higher energies. The length of the bubble is larger for a larger diameter of the fiber at the same energy setting of the laser.

In Fig 9, the development of the length of the bubble in time was determined for the 400 µm tip in the range of 25 to 250 mJ.

From the images and results in Figs 5 to 9, the following characteristics were observed:

- The beginning of the bubble starts earlier when the pulse energy is higher.
- The onset of the implosion is later.
- At higher pulse energies after implosion of the first bubble, a second bubble is visible that collapses later.
- At the same energy settings of the laser, the dimensions of the bubbles are larger for larger diameter fibers, indicating that the energy transfer through a smaller fiber is less.

Root Canal Model

Using the high-speed imaging setup as described, recordings were made with the two glass models of a root canal (Fig 10). Because of the diameter of the

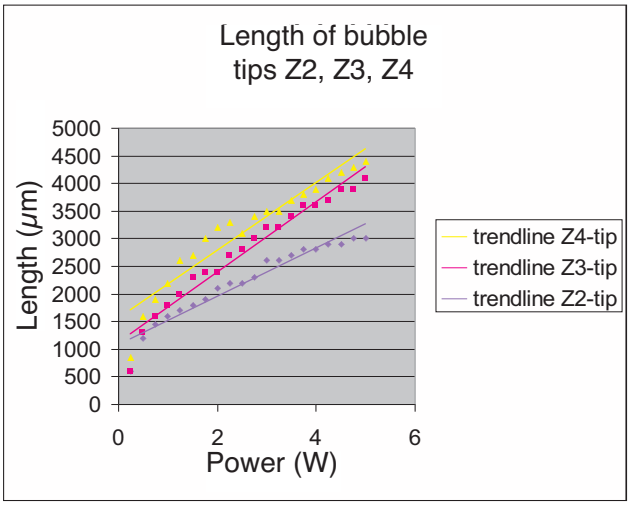

Fig 8 Length of the bubble vs power on the display of the laser at 20 Hz.

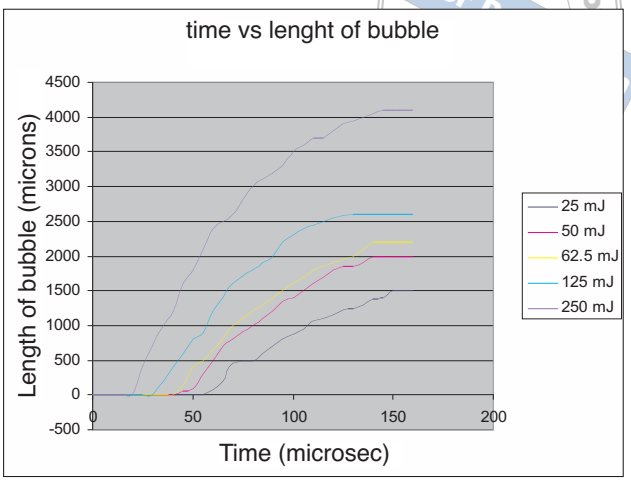

Fig 9 Development of bubble length in time for a 400-µm fiber for energies from 25 to 250 mJ.

canal, only 200 µm fibers were used. The glass models were submerged in water and the tip of the fiber was at a fixed position in the canal.

Similar to the previous experiments of the fiber in free water, individual images at each delay time are combined into sequences as shown in Figs 11 and 12, showing the dynamics during the lifetime of the expanding and imploding bubble inside the root canal model.

Compared to the bubble in a free water environment, the dynamics in the root canal are different due to the limited space inside the small canal (sees Fig 11 and 12, notice the air bubble already present in the canal). Typically, the dynamics of the bubble inside the canal can be described as follows:

During the interaction with the water during the exposure time of around 130 µs, water is turned into water vapor. The small canal, however, prevents the vapor from expanding freely laterally, pushing the water both forward and backward in the canal. The forward pressure can be easily observed in the first three frames of each sequence showing an air bubble, present in the canal, being compressed to a flat disk. Since the water obstructs the expansion of the vapor in the forward direction, the bubble also grows backwards along the fiber. The pressure inside the bubble remains high for a long time, since it has to fight against the resistance of the water which has to be displaced in the small canal. This process delays the dynamics of expansion and implosion compared to the free water situation. The process in the small canal takes about 3 times longer, as is illustrated in Fig 13. At the maximum expansion, almost the whole canal is filled with vapor (depending on the pulse energy). As already illustrated in Fig 4, the water (dye) is ejected from the canal exit at high speed. During implosion, the water is sucked back into the canal if water is present on top, otherwise air bubbles will also enter the canal. To make these experiments reproducible, we ensured that there was always water above the canal. During implosion, the air bubble that was pressed to the apex of the canal also expands to almost vacuum before water from the top streams back and thus contributes to the process of cavitations. Due to the resistance caused by the small diameter of the canal, which is also obstructed by the fiber itself, it takes time before the water has filled the gaps and the situation is stabilized. Depending on the pulse energy, this can take up to milliseconds.

The dynamics of bubble growth in the canal compared to the free water situation is illustrated in Figs 13a and 13b. The lateral and forward expansion is limited by the canal wall, while the backward expansion is blocked by the fiber making the lumen of the canal even smaller.

DISCUSSION

In this study, a better understanding of the mechanism of action of 2780 nm Er,Cr:YSGG laser pulses in a root canal model was obtained using high-speed imaging.

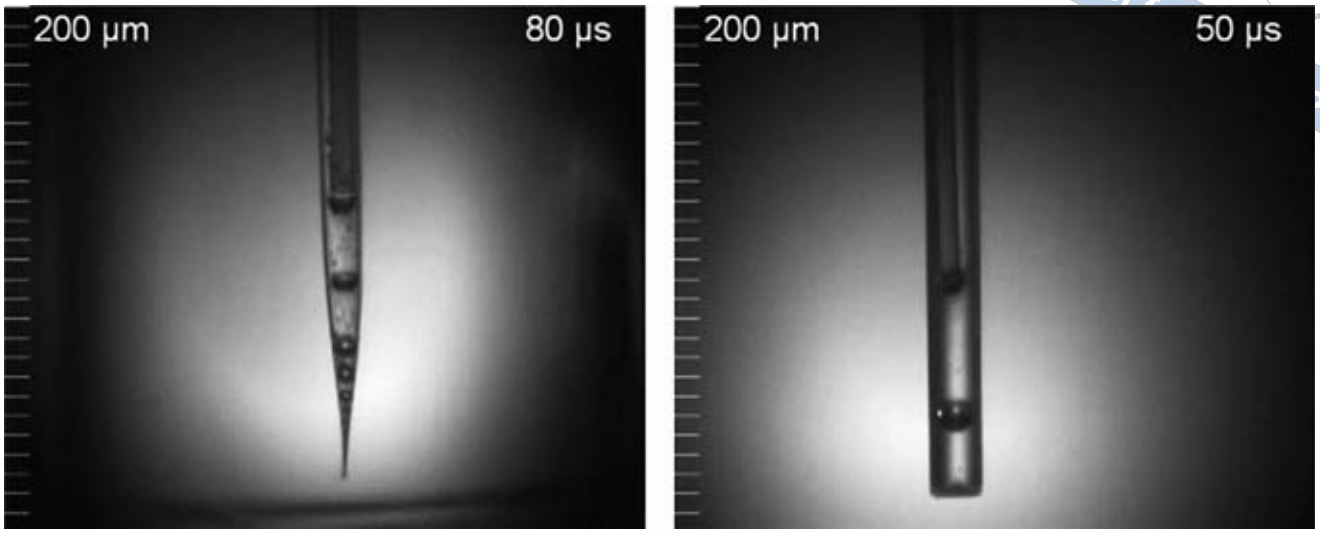

Fig 10 Examples of captured images of a bubble at the start of expansion in the conical (left) and cylindrical (right) root canal model.

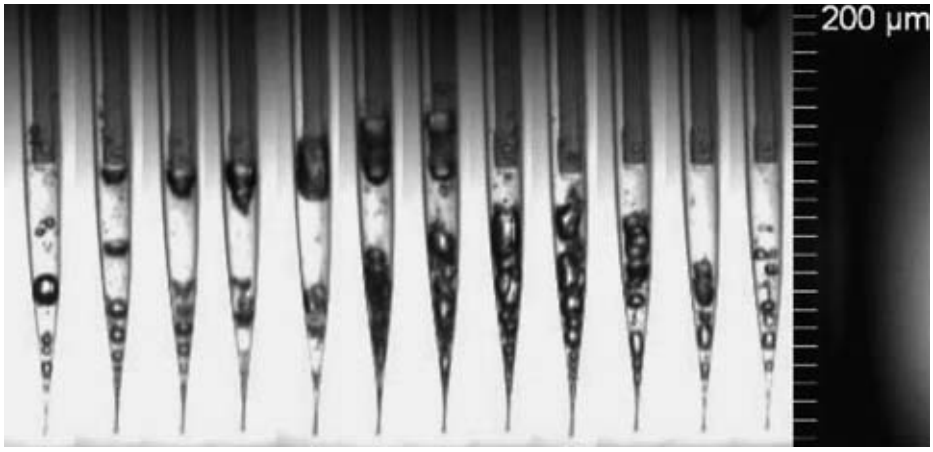

Fig 11 Captured images of expanding and imploding vapor bubble inside the conical root canal model at 50, 80, 90, 100, 130, 180, 210, 300, 450, 550, 660 and 720 µs after the onset of 12 mJ pulses at 20 Hz.

Due to the strong absorption of the Er,Cr:YSGG wavelength in water, the dynamics of water and water vapor are expected to play a major role in the mechanism of action treating and cleaning root canals. The high-speed imaging method as applied enables the capture of images with microsecond resolution. Although each image is captured from a different pulse of the laser, the dynamics of bubble formation has proven to be reproducible in the in vitro setting used for this study.

Vapor Bubble Dynamics

In order to understand the basics of water vapor expansion and implosion induced by a microsecond pulsed laser system, we performed imaging of the interaction of erbium laser pulses delivered through a fiber under water. It has provided an insight into the dependence of bubble size and life time on fiber size and pulse energy. This data could be used for comparison with the observed dynamics in the root canal model.

Presence of Water or Water Spray During Root Canal Treatment

Going from the free water situation to the root canal model, the assumption is made that there is always water present in the root canal. The tip of the laser system used is always used in combination with a water spray. The water fills the canal, although small air bub-

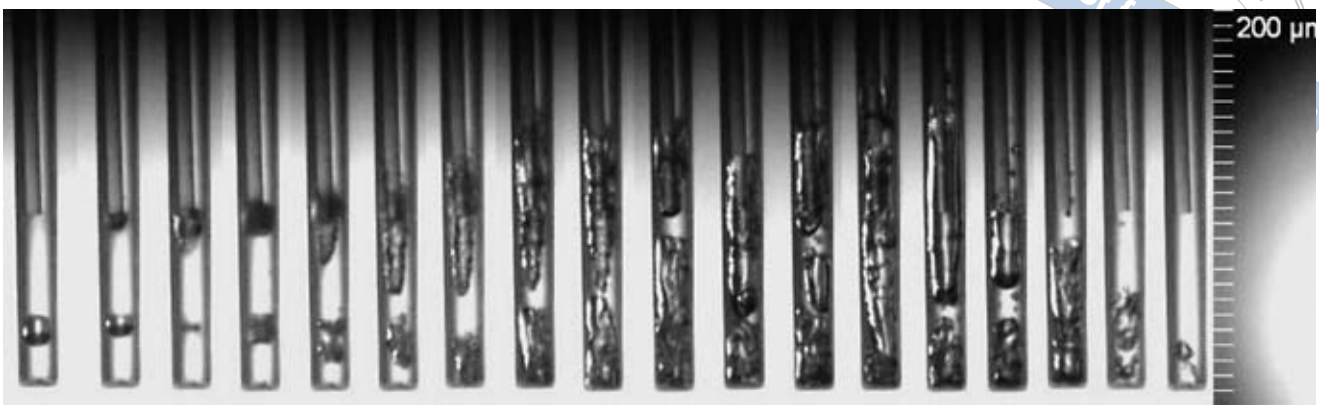

Fig 12 Captured images of expanding and imploding vapor bubble inside the cylindrical root canal model from 0 to 1200 µs after the onset of 50 mJ pulses.

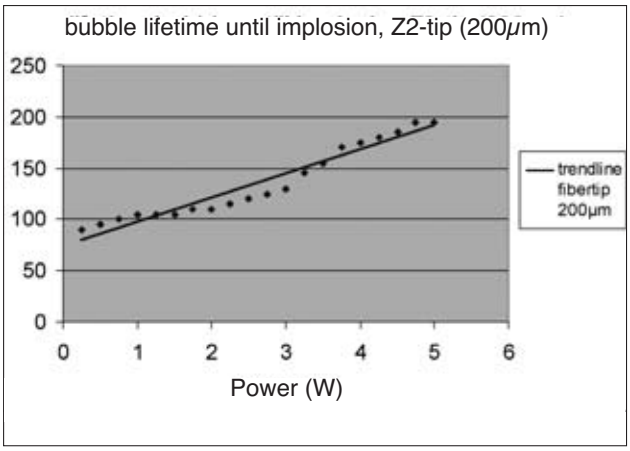

Fig 13a Lifetime of the vapor bubble in a free water situation until implosion, fiber Z2, 20 Hz.

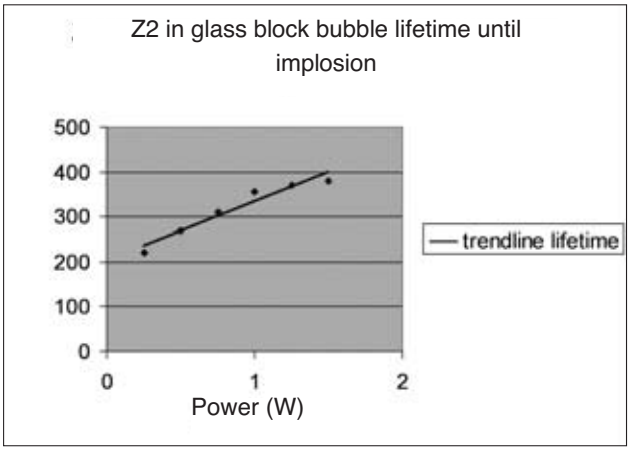

Fig 13b Lifetime of the vapor bubble in a glass block until implosion, fiber Z2, 20 Hz.

bles tend to remain in the canal as can be seen in Figs 11 and 12. During expansion, the water is ejected from the canal; however, during implosion, water from the spray is sucked back into the canal. This is clearly shown in Fig 4. At energy settings above 200 mJ, colored fluid in the canal was replaced by clear fluid within a few pulses.

In clinical settings, besides water, air bubbles also enter the canal. These air bubbles might contribute to the mechanism as described in the results. In our study, the root canal model was totally submerged in water to prevent air bubbles from coming in, which would interfere with the reproducibility of the images to create a sequence in time.

Despite this precaution, air bubbles appeared in the root canal after exposure to the laser. Air bubbles are attributed to gases dissolved in the water and come out of solution due to the large variation in phase pressures during the laser pulses. To minimize the occurrence of these gas bubbles, the water was boiled before the experiments to remove dissolved gases.

High-speed Water Motion and Cavitation

This study showed that fluid flushed at very high speed through the root canal created shear stresses on the wall. From the data in Fig 13, it can be calculated that during bubble expansion, fluid is pushed through the canal at speeds of tens of meters per second (up to 100 km/h). During implosion, the reverse will happen with comparable speeds. The shear stress along the wall of the canal should be sufficient to remove the smear layer and perhaps also remove infectious bacte-

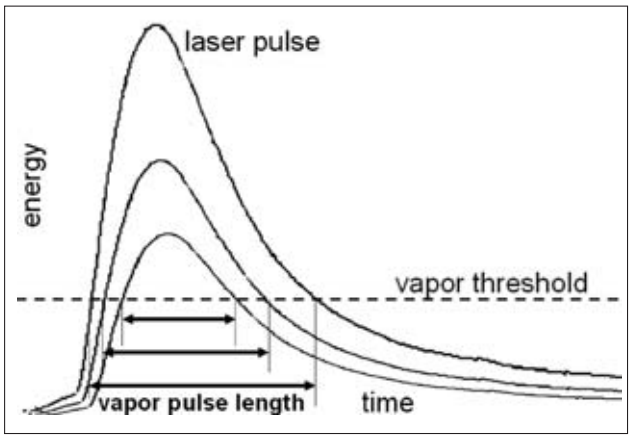

Fig 14 The temporal pulse profile of an Er,Cr:YSGG laser at different energy levels. Note that at higher pulse energies the vapor pulse length is increased, since the vapor threshold remains constant.

ria and biofilm. Additionally, this high-speed fluid motion induces secondary cavitation bubbles at irregularities along the wall. The implosion of the primary and secondary bubbles creates microjets in the fluid aimed at the wall with very high forces locally. This phenomenon is already applied in ultrasound baths for cleaning instruments. This mechanism might also contribute to the disruption of cells and the smear layer at the wall.

Bubbles Related to Pulse Shape

Bubble size and life cycle as they depend on energy can be explained by looking at the pulse characteristics of the laser. Figure 15 shows the typical temporal shape of the pulse of the Er,Cr:YSGG laser system used in this study (Waterlase Millenium). Depending on the fluence (mJ/mm^2) on the fiber surface, a layer of only a few µm of water in front of the fiber tip will turn to vapor as it is heated instantly to 100°C by absorption of the Er,Cr:YSGG laser light. This threshold for ablation is indicated in the temporal shape of the energy output of the laser pulse. The vapor bubble formed creates an opening in the water and the beam continues to vaporize the water and the interface between vapor and water in front of the fiber tip. This process continues as long as the energy level is above the ablation threshold of water. This could be defined as the ablation length, or vapor pulse length, of the laser pulse. For higher pulse energies, the level of ablation is reached faster and continues longer compared to lower pulses energies, as depicted in Fig 14.

Based on these pulse characteristics, the bubble dynamics (size and lifetime) presented, for instance, in Fig 8, can be understood. For lower energies, the threshold of ablation (= the moment of bubble formation) is reached later, and the energy drops below the threshold sooner compared to higher energies, explaining the starting time of bubble formation and length of the bubble.[16,17]

For higher energies, the steep rise of the energy in the pulse explains the fast growth in length of the bubble.

Energy and Fiber Diameter

Based on the explanation above, one would expect that the bubble would start faster for smaller fibers at equal energy settings due to the higher fluences (mJ/cm^2) at the fiber tip. However, the data show the opposite. Since the energy settings used in the experiments are the settings of the laser, the actual energy output was different due to losses of energy transfer for smaller diameter fibers. The manufacturer provides calibration correction figures for the different sizes of laser tips. These are:

400-µm tip = 0.75 (relative number)
300-µm tip = 0.60
200-µm tip = 0.30

The settings on the display have to be corrected by this factor to yield the pulse energy at the fiber tip.

For comparison of the bubble characteristics in relation to fiber diameter, the starting time for bubble formation is influenced by the fluence at the fiber surface and the corrected energy. For bubble length, it will mainly depend on corrected energy.

Impact of Vapor on Direct Laser Irradiation of Apex

The cavitation bubbles can be as long as 5 mm and up to 2.5 mm wide for a 400-µm tip. The bubble has a long, almost elliptical shape.

This might be a problem in a root canal where the apical constriction is an area that should be left intact. In a preliminary study, Matsuoka et al[18] found that to prevent damage to the apical area, they had to keep the 200- and 320-µm fibers 2 and 3 mm away from the anatomical apex. Since they used 2W power, their findings seem to be consistent with those from this study.

Future Studies

This study has provided an initial understanding of the mechanism of action of Er,Cr:YSGG laser pulses in root canal treatment. Evidently, more studies have to be performed to substantiate our hypothesis and include more factors of influence, such as temperature. Using a special thermal imaging setup, initial results have been obtained. It might also be interesting to repeat our experiments with a high-speed camera recording a single pulse in real time and to assess the effects of this laser on a smear layer and biofilm in vitro.

Our high-speed imaging setup may also be used to assess the altered bubble dynamics if the tip design is changed.

CONCLUSION

The high-speed imaging technique has provided sufficient data to support the following hypothesis: The mechanism of action during root canals treated with Er,Cr:YSGG laser pulses is based on rapidly expanding and imploding water vapor bubbles, creating high velocity water jets along the canal wall, removing the smear layer. Secondary cavitation effects also contribute to the cleaning and sterilization potential of the treatment.

High-speed imaging has proven useful in obtaining a better understanding of the mechanism of action of microsecond pulsed laser in the treatment of root canals.

ACKNOWLEDGMENTS

The authors want to thank Prof. Dr. Paul Wesselink and the students Tycho van Essen and Caroline Offerhaus from ACTA Dental School, Amsterdam; Hans van Heeswijk from the Fontys Hogeschool, Eindhoven, for their help during the laboratory work and data processing; Rick Mansveld from the Department of Biomedical Engineering of the University Medical Center in Utrecht for his help and cooperation; and Biolase Germany for lending the Er,Cr:YSGG laser.

REFERENCES

1. Moritz A, Gutknecht N, Goharkhay K, Schoop U, Wernisch J, Sperr W. In vitro irradiation of infected root canals with a diode laser: Results of microbiologic, infrared spectro-metric, and stain penetration examinations. Quintessence Int 1997;28:205-209.
2. Moritz A, Gutknecht N, Schoop U, Goharkhay K, Dörtbudak O, Sperr W. Irradiation of infected root canals with a diode laser in vivo: Results of microbiological examinations. Lasers Surg Med 1997;21:221-226.
3. Schoop U, Moritz A, Kluger W, et al. The Er:YAG laser in endodontics: results of an in vitro study. Lasers Surg Med 2002; 30:360-364.
4. Schoop U, Kluger W, Moritz A, et al. Bactericidal effect of different laser systems in the deep layers of dentin. Lasers Surg Med 2004;35:111-116.
5. Kimura Y, Wilder-Smith P, Matsumoto K. Lasers in endodontics: a review. Int Endod J 2000;33:173-185.
6. Yamazaki R, Goya C, Yu D, Kimura Y, Koukichi M. Effects of erbium,chromium:YSGG laser irradiation on root canal walls: a scanning electron microscopic and thermographic study. J Endod 2001;27:9-12.
7. Matsuoka E, Jayawardene JA, Matsumoto K. A morphological study on root canal preparation using erbium,chromium:ysgg laser. J Oral Laser Applic 2005;1:17-22.
8. Fried D, Featherstone JDB, Visuri SR, Seka W, Walsh JT. Caries inhibition potential of Er:YAG and Er:YSGG laser radiation. SPIE Proc 1996;2672:73-78.
9. Hossain M, Nakamura Y, Yamada Y, Kimura Y, Matsumoto N, Matsumoto K. Effects of Er,Cr:YSGG laser irradiation in human enamel and dentin: ablation and morphological studies. J Clin Laser Med Surg 1999;17:155-159.
10. Lauterborn W, Ohl C. Cavitation bubble dynamics. Ultrasonics Sonochemistry 1997;4:65-75.
11. Mrochen M, Riedel P, Donitzky C, Seiler T. Cavitation bubble formation during Erbium:YAG laser vitrectomy. Der Ophtalmologe 2001;98:163-167.
12. Levy G, Rizoiu I, Friedman S, Lam H. Pressure waves in root canals induced by Nd:YAG laser. J End 1996;22:81-84.
13. Verdaasdonk RM. In: Finlayson DM, Sinclair BD (eds). Advances in Lasers and Applications. Bristol: Institute of Physics Publishing, 1999:181-226.
14. Verdaasdonk RM, van Swol CFP, Grimbergen MCM, Rem AI. Imaging techniques for research and education of thermal and mechanical interactions of lasers with biological and model tissues. J Biomed Optics 2006;11:041110-1/1.
15. van Leeuwen TG, van der Veen MJ, Verdaasdonk RM, Borst C. Non contact tissue ablation by Holium:YSGG laser pulses in blood. Lasers Surg Med 1991;11:26-34.
16. Strassl M, Üblacker B, Bäcker A, Beer F, Moritz A, Wintner E. Comparison of the emission characteristics of three Erbium Laser Systems: a physical case report. J Oral Laser Applic 2004;4:263-270.
17. Grimbergen MCM, Verdaasdonk RM, van Swol CFP. Prediction of the ablation effect of ultra-pulsed CO_2 laser systems in clinical procedures. In: Jaques SL (ed). Laser-Tissue Interaction VIII. Proc SPIE 1997;2975:426-432.
18. Matsuoka E, Jayawardena JA, Matsumoto K. Morphological study of the Er,Cr:YSGG laser for root canal preparation in mandibular incisors with curved root canals. Photo Med Laser Surg 2005; 23:480-484.

Contact address: Jan Blanken, Bartoklaan 42, 3533 JA Utrecht, the Netherlands. Tel:+31-621-243-043, Fax: + 31-30-298-1414. e-mail: post@bartoklaan.nl or r.m.verdaasdonk-@umcutrecht.nl